INSTITUTE OF PHYSICS PUBLISHING JOURNAL OF PHYSICS B: ATOMIC, MOLECULAR AND OPTICAL PHYSICS

J. Phys. B: At. Mol. Opt. Phys. **36** (2003) 3303–3314 PII: S0953-4075(03)60553-5

Absolute cross sections for single and double charge-exchange in Fe^{q+} impacting on He

I Čadež[1,2], J B Greenwood[3], J Lozano[1], R J Mawhorter[1,4], M Niimura[1], S J Smith[1] and A Chutjian[1]

[1] Jet Propulsion Laboratory, California Institute of Technology, Pasadena, CA 91109, USA
[2] Jožef Stefan Institute, 1000 Ljubljana, Slovenia
[3] Physics Department, The Queen's University, Belfast BT7 1NN, UK
[4] Department of Physics and Astronomy, Pomona College, Claremont, CA 91711, USA

Received 4 March 2003, in final form 5 June 2003
Published 18 July 2003
Online at stacks.iop.org/JPhysB/36/3303

Abstract

We report measured absolute single and double charge-exchange cross sections (CSs) for Fe^{q+} ions with He at the ion impact energy of $7.0 \times q$ keV for $q = 5$–13. The range of ion velocities is 350 km s^{-1} for $q = 5$, to 560 km s^{-1} for $q = 13$, comparable to typical solar wind velocities. A retarding-field method is used for charge-state analysis of the ion beam after traversing the stationary target gas cell. The CSs are determined from absolute measurements of the ion currents and He target gas pressure.

1. Introduction

Highly charged Fe^{q+} ions are important heavy-ion constituents in the solar wind. These ions are present in charge states ranging from $q = 7$ to 13, with $q = 10$ and 11 being the most abundant in the fast solar wind, and $q = 9$ in the slow solar wind (von Steiger *et al* 2000a, 2000b, Wegmann *et al* 1998, Schwadron and Cravens 2000). Characteristic bulk solar wind velocities range from about 350 km s^{-1} to about 800 km s^{-1}. Charge-exchange collisions of solar-wind ions with atoms and molecules from cometary and planetary atmospheres lead to the emission of characteristic x-ray and UV photons. Knowing the cross sections (CSs) for these processes is therefore of importance for interpreting the observed spectra from different solar-system objects. Closer to home, Fe ions are present as impurities in fusion plasmas (Phaneuf *et al* 1987, Janev 1995). Their collisions with neutral atoms and molecules from the edge plasma are important for modelling the plasma-wall interaction.

He is an important neutral gas target. It is present in the solar corona, the atmospheres of the outer planets and fusion edge plasma. It also comprises about 10% of the interstellar gas (the remainder being atomic hydrogen), and its interaction with solar-wind ions is estimated to be the source of about 50% of the total soft background x-ray emission (Cravens 2000).

The possibility that these same x-ray mechanisms could occur in stellar winds interacting with neutral gas in the ambient interstellar medium, or even with a circumstellar cloud, has been used to lower the upper limit of the mass-loss rate from late-type dwarf stars by several orders of magnitude (Wargelin and Drake 2002). From a theoretical standpoint He is a relatively simple two-electron target, with a variety of studies available for multiple electron capture by highly charged ions (see, for example, Barat and Roncin 1992, Janev *et al* 1995).

In Fe^{q+}/He collisions different charge-changing processes can occur, and in general one can write

$$Fe^{q+} + He \rightarrow Fe^{(q-j)+} + He^{(j+s)+} + se \tag{1}$$

where j is the number of electrons captured by the projectile and s is the number of free electrons produced by the collision. For the two-electron He, $j = 0$, 1, or 2. In the present experiment we determine absolute charge-changing CSs which are the sum of the CSs for all channels with $j = 1$ ($\sigma_{q,q-1}$, single charge exchange) and $j = 2$ ($\sigma_{q,q-2}$, double charge exchange).

One-electron capture (single capture, SC) by highly charged ions (HCIs) predominantly occurs to a higher n-state of the projectile. This state is subsequently stabilized by photon emission. In the case of the two-electron capture one or both electrons may be in the excited states. The resulting doubly excited ion stabilizes either by autoionization (autoionizing double capture, ADC) or by photon emission ('true' double capture, TDC). Transfer ionization ($j = 1$ and $s = 1$, TI), SC and ADC all contribute to the single charge-exchange CS while only TDC contributes to the double charge-exchange CS.

Interest in charge-exchange collisions of Fe^{q+} with hydrogen and He has been sparked by fusion plasma research (Phaneuf *et al* 1987, Janev *et al* 1995). The absolute CS for one-electron capture by Fe^{q+} ions in hydrogen and/or He have been reported by Gardner *et al* (1977), Meyer *et al* (1979), Crandall *et al* (1980) and Phaneuf (1983). Through the analysis of experimental and theoretical results for different HCI/target combinations, general scaling rules for charge-exchange CS have been established for Fe ions by Phaneuf *et al* (1987), and summarized and extended to some additional cases by Janev *et al* (1995).

Absolute CSs are required for normalizing relative measurements, and for modelling different plasma environments. However, additional physical insight is gained by state-selective experimental studies. State-selective one-electron capture in collisions of low-energy Fe^{3+} and Fe^{4+} ions with H and He has been studied by McLaughlin *et al* (1993). These authors used translational energy spectroscopy to select the initial quantum state of the projectile ion. They showed that electron capture mainly occurs to the 3d and $n = 4$ states of the projectile. Energy-change spectra also showed the presence of metastable ions in the incident ion beam, especially for the Fe^{3+} case. Highly excited ions created by electron capture in ion–atom collisions have also been studied using photon emission spectroscopy. Druetta *et al* (1995) measured VUV emission CS for SC by $15q$ keV Fe^{7+}, Fe^{8+} ions in He and H_2. Wang *et al* (1997) studied photon emission from Fe^{7+} produced by one-electron capture of 80 keV Fe^{8+} ions on He and Ar. These authors identified 12 new transitions and seven new energy levels in Fe^{7+}. Such spectroscopic data are required not only in the fusion programme, but also for identifying the rich stellar spectra being detected by the new NASA and ESA satellite x-ray spectrometers (Ballantyne *et al* 2002, Ness *et al* 2002).

Recently, an experimental set-up was developed in our laboratory for measuring the absolute charge-exchange CS for cases of astrophysical importance (Greenwood *et al* 2000, 2001). Here we present the measured CS for single and double charge-exchange in collisions of Fe ions with He. Due to a very small double charge-exchange CS a new procedure was used to avoid the influence of two sequential one-electron capture collisions.

2. Experimental details

2.1. Experiment

The experimental apparatus for the charge-exchange studies is mounted on one of the beam lines at the JPL HCI facility (Chutjian *et al* 1999, Greenwood *et al* 2000), and is described in detail elsewhere (Greenwood *et al* 2001). The experimental configuration used here is shown in figure 1. The experimental set-up is housed inside a six-way cross pumped by a 250 l s^{-1} turbomolecular pump. For determining charge-exchange CS, a retarding field is used for charge-state analysis of the scattered ions. A well collimated, small-diameter beam of the desired projectile ion is passed through a cell containing the target gas. After traversing the cell, the ion beam is analysed by a retarding field. The transmitted ions are collected in a Faraday cup. By determining the absolute pressure (P_C) and temperature (T) of the target gas, measuring the absolute ion current ratios, and given the geometrical parameters, absolute CSs are given by

$$\sigma_{q,q-j} = \frac{J_j}{NLJ_0^0} = \frac{qI_j}{NL(q-j)I_0^0}. \tag{2}$$

Here J_0^0 and J_j are the particle currents of the incident Fe^{q+} and product $Fe^{(q-j)+}$ ions, respectively, and the corresponding measured electric currents are I_0^0 and I_j. In the present case $q = 5$–13 and $j = 1$ or 2. The target density is given as $N = P_C/kT$, and the path length through the target gas is denoted as L.

The projectile ions are extracted from a 14.5 GHz electron cyclotron resonance ion source (ECRIS). The ion feed gas used was pure ferrocene vapour [$Fe(C_5H_5)_2$)], a metal-organic compound having a vapour pressure at a room temperature that was high enough to ensure stable ion source operation. Ions of either isotope ^{56}Fe or ^{54}Fe were used as needed, to avoid any interference with the background ions at certain values of M/q. High-purity (99.997%) He was used throughout the measurements. The vacuum base pressure was 7×10^{-9} Torr and the corresponding background gas had a negligible effect on measured currents.

After extraction from the source the ions are filtered by a double focusing 90° bending magnet to obtain the desired M/q species. The beam is then steered into the charge-exchange beam line by a 45° 'Y' electrostatic deflector, focused by an electrostatic einzel lens system, and collimated by a set of four apertures. The electrostatic deflector and subsequent einzel lens are differentially pumped by a separate turbomolecular pump. Thus a narrow-diameter, collimated beam (0.7 or 1.2 mm in diameter for the two cell geometries used in the experiment) is introduced into the gas cell. The cell itself is 60.8 mm long with an ion-beam exit aperture diameter of either 2.54 or 4.09 mm.

Unscattered ions as well as ions forward-scattered into a small solid angle are transmitted through the cell and subsequently analysed by the retarding field. If the initial ion acceleration voltage is V_{acc} then the parent ions will be reflected by a retarding potential of the same value. Ions which have captured j electrons will be reflected by a potential higher than the critical value defined by $V_R = qV_{acc}/(q-j)$. Hence the retarded ion current will have a stepwise dependence on the retarding field. This allows a sequential filtering from the transmitted beam of ions of decreasing charge. The height of the current step at V_R is equal to the ion current I_{q-j}.

The target density is determined by measuring the absolute pressure P_B with a capacitance manometer. The measured pressure was corrected for the pressure drop between the gauge head and gas cell by calculating the tubing conductance. The correction factor was verified by calibration measurements with several different gas-cell conductances. The path length

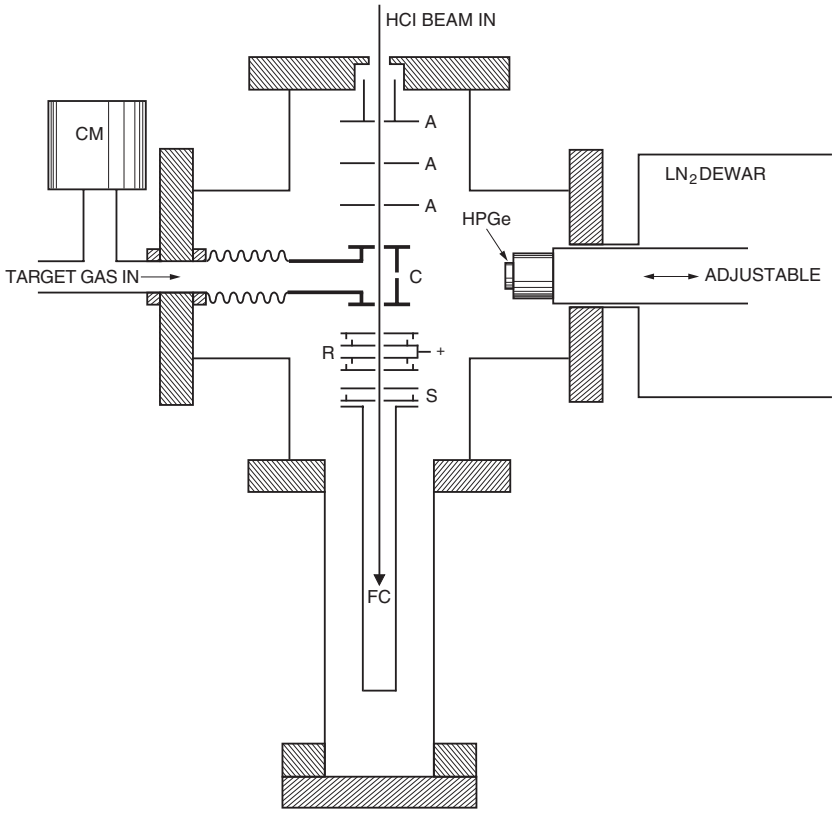

Figure 1. Schematic drawing of the experimental set-up used for the present measurements. The notation is: (A) three collimating apertures, (C) target gas cell, (R) retarding-field plates, (S) suppressor electrode, (FC) Faraday cup, (CM) capacitance manometer and (HPGe) x-ray detector for complementary studies (shown retracted, not used here).

L in equation (2) is corrected for the pressure increase outside the target cell due to the gas effused from the cell and the finite pumping speed of the experimental chamber containing the collimating apertures, target cell, retarding electrodes and ion collector (Čadež *et al* 2002).

Two procedures are used for the CS determinations. In the first, low, stable gas pressure is maintained in the cell, and the ion current is measured for different retarding fields. CSs are determined from equation (2). In the second procedure the ion current is recorded while the target gas pressure is slowly varied from zero to some low value, at various retarding potentials. We have extended this method herein by raising the upper limit of the target pressure to *higher* values where multiple collisions contribute to the detected current. All CSs are then determined by the self-consistent calculation of the beam attenuations, as described below.

The ion acceleration voltage for the present measurements is 7.0 kV. Due to the low target mass the largest kinematically possible scattering angle is rather small, $\theta_{\max} = 4.1°$. This kinematic condition enhances the strong forward-peaking of the scattered ion distribution, ensuring essentially total ion collection.

2.2. The influence of metastable ions

Ion beams extracted from an ECR ion source consist of a variety of HCIs in ground and excited electronic states. After extraction from the ECR the mass/charge selected ions travel 3 m to the

experimental target gas cell. The flight time for 7.0 kV extraction voltage ranges from 5.4 μs for Fe^{13+}, to 8.6 μs for Fe^{5+}. This time is sufficient for ions in dipole-connected transitions to decay before reaching the interaction region. Ions initially in metastable states, or which become metastable due to cascading from higher states, may be present in the incident ion beam.

In order to assess and minimize the presence of metastable ions in the incident beam different procedures and checks were applied. For some measurements the ECR was operated at relatively high pressures. Our previous experience has shown that this effectively quenches any metastable ions in the plasma and extraction regions. Such quenching was monitored for several Fe charge states by detecting photon emission from the low-lying metastable states using a Kingdon ion trap in a separate beam line to trap the metastable ions (Smith *et al* 1999). No emission from metastable states could be detected when the ECR was run in a high-pressure mode. Hence the charge-exchange CS measured under higher-pressure ECR conditions should be free of metastable states. Interestingly, it was also found that CS measured under lower-pressure conditions, where metastables could be detected in the Kingdon trap line, agreed with those measured under the higher-pressure mode. Two possible explanations for this effect are (a) the charge-exchange CS from the ground and low-lying metstable states at these high-charge states are effectively the same (within experimental error), or (b) a different spatial distribution of ions exists at the ECR, with the central, more collimated beam used in the charge-exchange measurements having a negligible metastable content.

Three additional checks on the possible influence of metastable ions were performed.

- Ion-beam attenuation measurements were carried out in the target gas cell. The observed current versus target gas pressure had simple, single-exponential dependence, with no breaks in the slope. One would expect such breaks if metastable ions were present and had a charge-exchange CS that was significantly different from that of the ground state.
- Secondly, approximately 5×10^{-6} Torr of Ar was introduced into a 0.7 m section of the beam line between the 90° bending magnet and the electrostatic 'Y' deflector. Measurements made with and without the quenching gas found no changes in the charge-exchange CS for the Fe^{9+} projectile ion.
- Finally, Fe^{8+} ions were deliberately produced by charge-exchanging Fe^{9+} ions on Ar in the magnet-to-'Y' region noted above. As the excited levels were populated by capture followed by cascade rather than electron impact ionization, these Fe^{8+} ions would have a different distribution of excited states than the Fe^{8+} ions extracted directly from the ECR ion source. Energy-equivalent measurements found no difference in the charge-exchange CS for these two different sources of incident ions. The same results were obtained using Fe^{7+} produced from Fe^{8+}.

These experimental checks are consistent with hypotheses (a) and (b) above, and taken together with the self-consistent fitting of the attenuation scans as described below, ensure that the possible influence of the metastable ions, if present, is within the experimental error of the measurements.

2.3. The model for data analysis

The method of analysis given in the appendix was used in those cases where data were taken in the varying-pressure mode. Using this method one uses the following conditions.

- One is not restricted to the single-collision regime. This leads to exponential expressions for ion currents as a function of gas cell pressure. Although the mathematical model

is general, for the present CS range only ions from single and double collisions make significant contributions to measured currents. However, triple collisions produce the dominant contribution to the ion current measured at V_g above the third threshold. The present method of analysis is necessary for measurements of very small double charge-exchange CSs. In these cases it is difficult to establish a clear linear region for a double charge-changed ion current versus target gas pressure.

- Only one value for the charge-exchange CS is assumed for each ion species independent of whether it is an incident ion or an ion produced by electron capture in the target cell. Hence ground- and excited-state ions present in both the primary and the charge-exchanged beams are treated equivalently. An inconsistency in the fitting of the charge-exchange currents versus pressure data would indicate that this assumption is weak and that additional charge-exchange reaction channels should be considered.
- Angular broadening effects by elastic or inelastic scattering, collisional ionization, ion-focusing by the retarding grids and the angular acceptance of the exit optics and Faraday cup do not essentially limit the full collection of the charge-exchanged ions.
- The target gas density is assumed to be homogeneous. Small inhomogeneities at the cell entrance and exit are compensated by using a longer effective path length for the cell.
- Since the gas target is He at most only two electrons may be captured by the projectile in a single collision. Naturally, more than two electrons can be exchanged under multiple-collision conditions.

Under these conditions there are exponential expressions for the different ion currents versus target pressure. Details of the derivations are given in the appendix. Combining the expressions for parent ions and ions with single, double and triple charge-exchange we can directly compare the model with the experimental variation of the ion currents for the extended pressure range, beyond the single-collision regime. In this fitting procedure, the CSs are used as parameters.

An example of the ion current variation with pressure for an 84 keV Fe^{12+} incident ion beam is shown in figure 2. With a 6.0 kV retarding potential all ions are transmitted by the retarding grids. The current attenuation is due to both single and double charge-changing collisions resulting in transitions to Fe^{11+} and Fe^{10+}. At a higher retarding potential of $V_R = 7.4$ kV, parent Fe^{12+} ions are stopped, and the measured current is produced by both Fe^{11+} and Fe^{10+} ions. At a still higher value of $V_R = 8.0$ kV only Fe^{10+} can penetrate the potential barrier and contribute to the measured current. Finally, at the highest retarding potential of $V_R = 8.8$ kV no ions should be present as He has only two electrons and hence Fe^{9+} cannot be produced in a single collision. However, if the target gas pressure is increased further, then ions from double and, to a lesser extent, triple collisions also contribute to the measured current. This effect produces a departure from the linearity of the measured current versus P_C, and the observed current for $V_R = 8.8$ kV is entirely due to double and triple collisions. The lines through the experimental data points are the results of the calculated attenuation using the derived CS set.

3. Results and discussion

The present experimental results for the single charge-exchange $Fe^{q+} \rightarrow Fe^{(q-1)+}$ and the double charge-exchange $Fe^{q+} \rightarrow Fe^{(q-2)+}$ are shown in table 1 and figure 3. The total absolute error in the measured CS is discussed in detail in Greenwood *et al* (2001) and Čadež *et al* (2002). Its components are (i) errors in the determination of ion currents, target density and cell path length; (ii) statistical errors of individual measurements; and (iii) possible systematic errors, for example, the presence of metastable states.

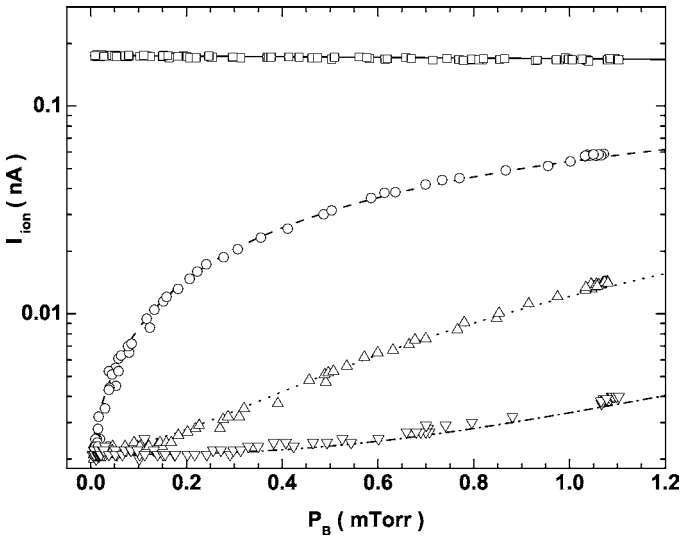

Figure 2. Ion current variation with target gas pressure for 84 keV $^{56}Fe^{12+}$ in He. Retarding voltage for individual curves are: 6.0 (□), 7.4 (○), 8.0 (△) and 8.8 (▽) kV. The model currents are represented by the lines through the experimental points.

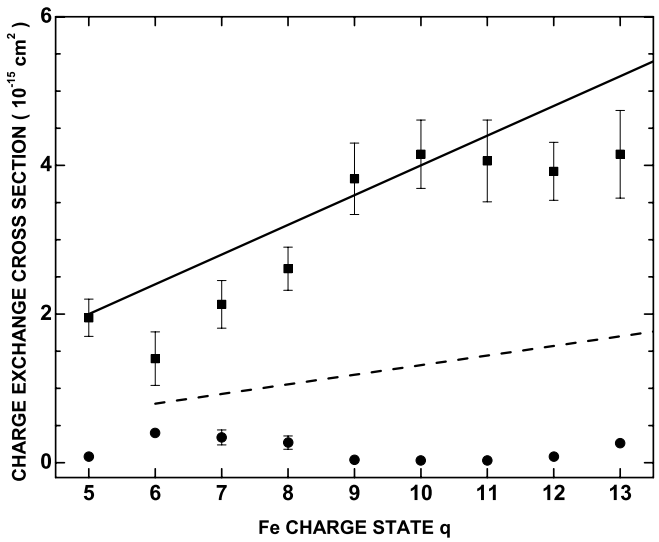

Figure 3. Measured single (■) and double (●) charge-exchange CS for Fe^{q+} on He. Also shown are the scaled estimated CSs for one-electron capture (——) and two electron processes (- - - -) according to Janev *et al* (1995).

The method used relies on the measurement of current ratios. Ion currents were measured with the same instrument on the same range setting. The error in gas-density determination arises from instrumental accuracies, the conductance pressure-correction factor, and uncertainty in the gas temperature. The target path length is taken to be the geometrical length of the target gas cell, with a correction for streaming through the apertures, and for the increased background pressure when gas is introduced into the target cell (Čadež *et al* 2002).

Table 1. $\sigma_{q,q-1}$ and $\sigma_{q,q-2}$ for Fe^{q+} on He at $7.0 \times q$ keV incident ion energy.

q	E_i (keV)	$\sigma_{q,q-1}$ (10^{-16} cm^2)	$\sigma_{q,q-2}$ (10^{-16} cm^2)
5	35	19.5 ± 2.5	0.8 ± 0.1
6	42	14.0 ± 3.6	4.0 ± 0.6
7	49	21.3 ± 3.2	3.4 ± 1.1
8	56	26.1 ± 2.9	2.7 ± 0.9
9	63	38.2 ± 4.8	0.4 ± 0.2
10	70	41.5 ± 4.6	0.3 ± 0.1
11	77	40.6 ± 5.5	0.3 ± 0.3
12	84	39.2 ± 3.9	0.8 ± 0.8
13	91	41.5 ± 5.9	3.0 ± 0.6

These uncertainties combined lead to a total instrumental error in the charge-exchange CS of 7.2% at the 95% (2σ) confidence level.

The main source of error in the determination of the charge-exchange CS is the limited reproducibility of individual measurements due to fluctuations in the ion beam. One source of *systematic* error is incomplete collection of the full angular distribution of the scattered ions. This can arise through a limiting cell-exit orifice, defocusing characteristics of the retarding field grids, and a limiting Faraday cup acceptance solid angle. We estimate that due to the large mass difference between the projectile ($M = 56$) and target atom ($M = 4$) these errors are negligible. This is confirmed by the consistency of our data taken with two different exit orifices. The total estimated errors for the present measurements are presented in table 1 and reflected in figure 3. These errors are 2σ statistical errors added in quadrature with the 7.2% instrumental error. They reflect the number of measurements taken for each charge state, as well as the reproducibility of the measurements. In three cases ($q = 6, 9$, and 11) the error bars were increased slightly to account for an additional error arising from the use of two different experimental techniques.

Although there are no equivalent experimental results with which to compare there is copious experimental, semiempirical and theoretical evidence that certain regularities and scaling relationships exist. For higher q valued CSs it has been shown (Janev *et al* 1995) that one- and two-electron capture do not depend strongly on the projectile ion or its core, that CSs scale linearly with q, and that the energy dependence of CSs is weak at low energies. A general scaling relationship was established for higher q values in the form $\sigma/q = f(\frac{E}{M\sqrt{q}})$, where $f(\frac{E}{M\sqrt{q}})$ contains constants derived from both experimental and theoretical studies.

For one-electron capture (SC) in He it has been shown (Phaneuf *et al* 1987, Janev *et al* 1995) that for $q \geqslant 5$, the CSs are approximately $4q \times 10^{-16}$ cm^2, independent of the projectile ion. This is valid for energies below $\sqrt{q}$ keV u^{-1}. This approximate CS is shown as the solid line in figure 3.

A simple scaling relationship has also been established for the sum of two-electron processes, double electron capture to both stable and autoionizing states as well as transfer ionization, i.e. TDC + ADC + TI (equation (25) of Janev *et al* 1995). This scaling relationship is shown as the dashed line in figure 3. However, only TDC manifests itself as the measured double charge-exchange CS while ADC and TI both contribute together with SC to the measured single charge-exchange CS.

When considered as a function of ion charge, the measured single charge-exchange CS indicates oscillatory behaviour about the smooth linear increase predicted by the scaled CS. Kim *et al* (1978) observed oscillations in the total electron-capture CS for several fast ($v > 1$ au)

heavy HCIs incident on atomic H. This was attributed to an interference effect between the long range and short range (screened) Coulomb potentials acting on the captured electron. Ryufuku *et al* (1980) studied charge transfer in a lower energy regime (<10 keV u^{-1}) for lighter ions. Oscillations were observed due to the crossings of diabatic potential curves, and were modelled reasonably well by the classical over-barrier model. In the present experiment, the additional observation of the oscillatory behaviour of the TDC CS shows that the oscillations in the single charge-exchange CS can be a consequence of the varying contributions of the ADC.

The present results show this interplay between single (SC + TI + ADC) and double (TDC) charge-exchange CSs. Higher double charge-exchange CS for $q = 6$–8 mirror the relative dip in the single charge-exchange CS, indicating a smaller contribution of ADC to the latter. However, this relative dip is about twice the corresponding increase of the double charge-exchange CS. The branching ratio for autoionization to radiative decay will determine how much of the initial DC contributes to the single or double charge-exchange CS, respectively. This in turn will depend on the initial states into which the two electrons are captured. If they are in nearly equivalent states $nln'l'$ (where $n \approx n'$) autoionization is dominant as the electron orbitals overlap, while for non-equivalent configurations $nln'l'$ ($n \ll n'$) radiative decay plays a more important role (see e.g. Barat and Roncin (1992) and references therein).

In studying DC from He using O^{6+} and Ne^{10+} at velocities below 1 au, Chesnel *et al* (1999) emphasize the difference between monoelectronic and dielectronic processes. The former, involving sequential capture of two electrons, will populate near-equivalent energy levels. For the latter the capture of two electrons simultaneously results in non-equivalent configurations due to an autoexcitation process involving the two correlated electrons. However, even if the two electrons are initially captured into a near-equivalent configuration, post-collision configuration interactions can result in a non-equivalent final state. Our results show that the DC for $q = 6, 7, 8$ must be into non-equivalent configurations as has been seen in collisions of O^{6+} with He (Chesnel *et al* 1999). For the higher charge states ($q = 9, 10, 11$) the electrons appear to be sequentially captured into near-equivalent levels which decay exclusively by autoionization. Here, the single charge-exchange CS is slightly above the $4q$ line. Thus one-electron capture is only about 80% of its scaled value if all the scaled DC would result in transfer ionization. The interplay between two CSs seems to return for $q \geqslant 12$.

We have studied the capture of one and two electrons from He for a range of incident Fe charge states. For single exchange resulting from one-electron capture, transfer ionization and autoionizing two-electron capture, the CS increases roughly linearly with the charge state. However, deviations from this trend are seen to correlate with an increase in the double charge-exchange CS due to radiatively stabilized DC. This contribution to double exchange depends critically on the doubly excited state of the ion following DC and on the branching ratio for autoionization and radiative decay. For low-charge states radiative stabilization is high, suggesting that non-equivalent states are being populated, while for high-charge states autoionization dominates and the double exchange CS is essentially zero.

Acknowledgments

I Čadež, M Niimura and R J Mawhorter all thank the National Research Council for Senior NRC Fellowships through the NASA-NRC programme. This work was carried out at the Jet Propulsion Laboratory, California Institute of Technology and was supported through agreement with the National Aeronautics and Space Administration.

Appendix

In order to carry through the analysis of the pressure dependence of a charge-exchanged signal we introduce the following notation: q refers to the charge state of the parent ion, j is the number of captured electrons, J_j are the particle currents, and $I_j = (q - j)J_j$ are the corresponding electrical currents. In addition, we introduce the sum S_{q-j} over lower charge-state CSs as $S_{q-j} = \sum_{i>j} \sigma_{q-j,q-i}$. Here, $\sigma_{q-j,q-i}$ is the CS for the $q - j \to q - i$ charge-state transition.

For the attenuation of the parent ion current ($j = 0$) one gets

$$\frac{1}{N}\frac{\mathrm{d}J_0}{\mathrm{d}x} = -J_0 S_q \qquad \text{and} \qquad J_0^f = J_0^0 \exp(-\alpha_0), \tag{A.1}$$

where x is coordinate along the ion beam, J_0^f is the parent ion current exiting the gas cell, and $\alpha_j = NLS_{q-j}$. From equation (A.1) in the low-density limit ($\alpha_J \ll 1$) one has $J_0^f = J_0^0(1 - \alpha_0) = J_0^0(1 - NLS_0)$.

For all $j > 0$, the steady-state population J_j results from formation by electron capture to ions in higher charged states, and loss by electron capture to ions of lower charge states. For J_1 one obtains

$$\frac{1}{N}\frac{\mathrm{d}J_1}{\mathrm{d}x} = J_0\sigma_{q,q-1} - J_1 S_{q-1}. \tag{A.2}$$

This simple inhomogeneous differential equation has the solution,

$$J_1^f = C_{11}[\exp(-\alpha_0) - \exp(-\alpha_1)] \qquad \text{with } C_{11} = J_0^0 \frac{\sigma_{q,q-1}}{S_{q-1} - S_q}, \tag{A.3}$$

using the initial condition that $J_1 = 0$ at $x = 0$. In the limiting case $P_C \to 0$ one has

$$J_1^f = J_0^0 NL\sigma_{q,q-1}. \tag{A.4}$$

The procedure can be continued and for J_2 one obtains

$$\frac{1}{N}\frac{\mathrm{d}J_2}{\mathrm{d}x} = J_0\sigma_{q,q-2} + J_1\sigma_{q-1,q-2} - J_2 S_{q-2}, \tag{A.5}$$

and

$$J_2^f = C_{21}[\exp(-\alpha_0) - \exp(-\alpha_2)] + C_{22}[\exp(-\alpha_1) - \exp(-\alpha_2)], \tag{A.6}$$

where C_{21} and C_{22} are now

$$C_{21} = \frac{J_0^0\sigma_{q,q-2} + C_{11}\sigma_{q-1,q-2}}{S_{q-2} - S_q}, \tag{A.7}$$

and

$$C_{22} = -C_{11}\frac{\sigma_{q-1,q-2}}{S_{q-2} - S_{q-1}}. \tag{A.8}$$

Again in the limiting case $P_C \to 0$ one gets

$$J_2^f = J_0^0 NL\sigma_{q,q-2}. \tag{A.9}$$

Finally, for the case of J_3 one has

$$\frac{1}{N}\frac{\mathrm{d}J_3}{\mathrm{d}x} = J_0\sigma_{q,q-3} + J_1\sigma_{q-1,q-3} + J_2\sigma_{q-2,q-3} - J_3 S_{q-3} \tag{A.10}$$

and

$$\begin{aligned} J_3^f = {} & C_{31}[\exp(-\alpha_0) - \exp(-\alpha_3)] + C_{32}[\exp(-\alpha_1) - \exp(-\alpha_3)] \\ & + C_{33}[\exp(-\alpha_2) - \exp(-\alpha_3)], \end{aligned} \tag{A.11}$$

where C_{31}, C_{32} and C_{33} are

$$C_{31} = \frac{\sigma_{q,q-3} J_0^0 + \sigma_{q-1,q-3} C_{11} + \sigma_{q-2,q-3} C_{21}}{S_{q-3} - S_q}, \tag{A.12}$$

$$C_{32} = \frac{-\sigma_{q-1,q-3} C_{11} + \sigma_{q-2,q-3} C_{22}}{S_{q-3} - S_{q-1}} \tag{A.13}$$

and

$$C_{33} = \frac{-\sigma_{q-2,q-3}(C_{21} + C_{22})}{S_{q-3} - S_{q-2}}. \tag{A.14}$$

Finally, for the weak absorption limit $P_C \to 0$, one has

$$J_3^f = J_0^0 NL\sigma_{q,q-3} = 0, \tag{A.15}$$

since $\sigma_{q,q-3} = 0$ for the two-electron He atom.

Operationally, the measured quantities are the ion currents (electrical) for the following increasing retarding voltage steps: (a) no ions are retarded and all charge states are passed; (b) only the parent ions are retarded; (c) parents and single charge-exchanged ions are retarded; (d) and finally parents, single-exchanged and double-exchanged ions are retarded. The currents are indexed as I_a, I_b, I_c and I_d, and are given by the following expressions

$$I_a = q J_0^f + (q-1) J_1^f + (q-2) J_2^f + \cdots, \tag{A.16}$$

$$I_b = (q-1) J_1^f + (q-2) J_2^f + \cdots, \tag{A.17}$$

$$I_c = (q-2) J_2^f + (q-3) J_3^f + \cdots \tag{A.18}$$

and finally

$$I_d = (q-3) J_3^f + \cdots. \tag{A.19}$$

The procedure can be continued by taking into account higher corrections. This is not needed for the present experimental conditions of CS, cell length and target pressure. Multiple collisions would also induce a larger angular spread of the exit beam, further complicating the simple model given in section 2.3.

The model currents, (A.16)–(A.19), after being normalized and adjusted to the experimental parameters (incident parent ion current I_0^0, instrumental zeros and pressure correction factor), are compared to the experimental data as shown in figure 2.

References

Ballantyne D R, Ross R R and Fabian A C 2002 *Mon. Not. R. Astron. Soc.* **336** 867

Barat M and Roncin P 1992 *J. Phys. B: At. Mol. Opt. Phys.* **25** 2205

Čadež I, Greenwood J B, Chutjian A, Mawhorter R J, Smith S J and Niimura M 2002 *J. Phys. B: At. Mol. Opt. Phys.* **35** 2515

Chesnel J-Y, Fremont F, Sulik B, Ruiz-Menendez C, Merabet H, Bedouet C, Husson X, Grether M and Stolterfoht N 1999 *Nucl. Instrum. Methods* B **154** 142

Chutjian A, Greenwood J B and Smith S J 1999 *Applications of Accelerators in Research and Industry (AIP Conf. Proc. vol 475)* ed J L Duggan and I L Morgan (New York: American Institute of Physics)

Crandall D H, Phaneuf R A and Meyer F W 1980 *Phys. Rev.* A **22** 379

Cravens T E 2000 *Astrophys. J.* **532** L153

Druetta M, Hitz D and Jettkant B 1995 Atomic and plasma-material interaction data for fusion *J. Nucl. Fusion (Suppl.)* **6** 225

Gardner L D, Bayfield J E, Koch P M, Kim H J and Stelson P H 1977 *Phys. Rev.* A **16** 1415

Greenwood J B, Chutjian A and Smith S J 2000 *Astrophys. J.* **529** 605

Greenwood J B, Williams I D, Smith S J and Chutjian A 2001 *Phys. Rev.* A **63** 062707

Janev R K (ed) 1995 *Atomic and Molecular Processes in Fusion Edge Plasmas* (New York: Plenum)

Janev R K, Winter H-P and Fritsch W 1995 *Atomic and Molecular Processes in Fusion Edge Plasmas* ed R K Janev (New York: Plenum) p 341
Kim H J *et al* 1978 *Phys. Rev. Lett.* **40** 1635
McLaughlin T K, Hodgkinson J M, Tawara H, McCullough R W and Gilbody H B 1993 *J. Phys. B: At. Mol. Opt. Phys.* **26** 3587
Meyer F W, Phaneuf R A, Kim H J, Hvelplund P and Stelson P H 1979 *Phys. Rev.* A **19** 515
Ness J U, Schmitt J H M M, Burwitz V, Mewe R and Predehl P 2002 *Astron. Astrophys.* **387** 1032
Phaneuf R A 1983 *Phys. Rev.* A **28** 1310
Phaneuf R A, Janev R K and Hunter H T 1987 *Nucl. Fusion (Special Suppl.)* 7
Ryufuku *et al* 1980 *Phys. Rev.* A **21** 745
Schwadron N A and Cravens T E 2000 *Astrophys. J.* **544** 558
Smith S J, Chutjian A and Greenwood J B 1999 *Phys. Rev.* A **60** 3569
von Steiger R *et al* 2000a *J. Geophys. Res.* **105** 27
von Steiger R *et al* 2000b *J. Geophys. Res.* **105** 217
Wang M, Arnesen A, Dunne P, Hallin R, Heijkenskjöld F and O'Reilly F 1997 *Phys. Scr.* T **73** 77
Wargelin B F and Drake J J 2002 *Astrophys. J.* **578** 503
Wegmann R, Schmidt H U, Lisse C M, Dennerl K and Englhauser J 1998 *Planet. Space Sci.* **46** 603